

From Macrocycles to Quantum Rings:

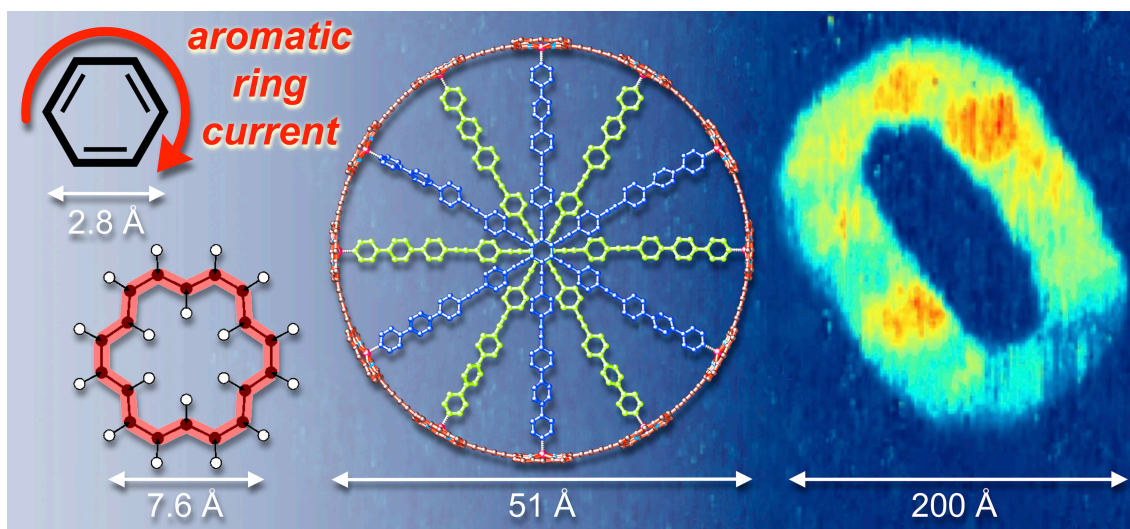
Does Aromaticity Have a Size Limit?

Michael Jirásek,^{,†,‡} Harry L. Anderson,^{*,†} and Martin D. Peeks^{*,#}*

[†]Department of Chemistry, University of Oxford, Oxford OX1 3TA, U.K.

[‡]Laboratory of Organic Chemistry, ETH Zurich, 8093 Zurich, Switzerland

[#]School of Chemistry, University of New South Wales, Sydney NSW 2052, Australia



CONSPECTUS: The ring currents of aromatic and antiaromatic molecules are remarkable emergent phenomena. A ring current is a quantum mechanical feature of the whole system and its existence cannot be inferred from the properties of the individual components of the ring. Hückel's rule states that when an aromatic molecule with a circuit of $[4n+2]$ π -electrons is placed

in a magnetic field, the field induces a ring current that creates a magnetic field opposing the external field inside the ring. In contrast, antiaromatic rings with $4n$ π -electrons exhibit ring currents in the opposite direction. This rule bears the name of Erich Hückel and it grew from his molecular orbital theory, but modern formulations of Hückel's rule incorporate contributions from others, particularly William Doering and Ronald Breslow. It is often assumed that aromaticity is restricted to small molecular rings with up to about 22 π -electrons. This Account outlines the discovery of global ring currents in large macrocycles with circuits of up to 162 π -electrons. The largest aromatic rings yet investigated are cyclic porphyrin oligomers, which exhibit global ring currents after oxidation, reduction or optical excitation, but not in the neutral ground state. The global aromaticity in these porphyrin nanorings leads to experimentally measurable aromatic stabilization energies, in addition to magnetic effects that can be studied by NMR spectroscopy. Wheel-like templates can be bound inside these nanorings, providing excellent control over the molecular geometry and allowing the magnetic shielding to be probed inside the nanoring. The ring currents in these systems are well reproduced by density functional theory (DFT), although the choice of DFT functional often turns out to be critical. Here we review recent contributions to this field, and present a simple method for determining the ring current susceptibility (in nA/T) in any aromatic or antiaromatic ring from experimental NMR data, by classical Biot-Savart calculations. We use this method to quantify the ring currents in a variety of aromatic rings. This survey confirms that Hückel's rule reliably predicts the direction of the ring current, and it reveals that the ring current susceptibility is surprisingly insensitive to the size of the ring. The investigation of aromaticity in even larger molecular rings is interesting because ring currents are also observed when mesoscopic metal rings are placed in a magnetic field at low temperatures. The striking similarity between ring currents in molecules and in

mesoscopic metal rings arises because the effects have a common origin: a field-dependent phase-shift in the electronic wavefunction. The main difference is that the magnetic flux through mesoscopic rings is much greater, owing to their larger areas, so their persistent currents are nonlinear and oscillatory with applied field, whereas the flux through aromatic molecules is so small that their response is approximately linear in applied field. We discuss how nonlinearity is expected to emerge in large molecular nanorings at high magnetic fields. The insights from this work are fundamentally important for understanding aromaticity and for bridging the gap between chemistry and mesoscopic physics, potentially leading to new functions in molecular electronics.

1. KEY REFERENCES

- Peeks, M. D.; Claridge, T. D. W.; Anderson, H. L. Aromatic and antiaromatic ring currents in a molecular nanoring. *Nature* **2017**, *541*, 200–203.¹ NMR spectroscopy and magnetic susceptibility results are presented demonstrating that a 6-porphyrin nanoring is globally antiaromatic in its 4+ oxidation state, globally aromatic in the 6+ oxidation state and locally antiaromatic in the 12+ oxidation state.
- Rickhaus, M.; Jirasek, M.; Tejerina, L.; Gotfredsen, H.; Peeks, M. D.; Haver, R.; Jiang, H.-W.; Claridge, T. D. W.; Anderson, H. L. Global aromaticity at the nanoscale. *Nat. Chem.* **2020**, *12*, 236–241.² ¹H, ¹³C and ¹⁹F NMR spectroscopy are used to characterize the aromatic and antiaromatic ring currents in a wide variety of porphyrin nanorings, in various oxidation states.
- Judd, C. J.; Nizovtsev, A. S.; Plougmann, R.; Kondratuk, D. V.; Anderson, H. L.; Besley E.; Saywell, A. Molecular quantum rings formed from a π -conjugated macrocycle. *Phys. Rev. Lett.* **2020**, *125*, 206803.³ The electronic structure of a 40-porphyrin nanoring is

characterized via scanning tunneling microscopy and scanning tunneling spectroscopy, on a silver surface at ~ 78 K, demonstrating that this nanoring has the potential to act as a molecular quantum ring.

- Jirásek, M.; Rickhaus, M.; Tejerina, L.; Anderson, H. L. Experimental and theoretical evidence for aromatic stabilization energy in large macrocycles. *J. Am. Chem. Soc.* **2021**, *143*, 2403–2412.⁴ Analysis of the oxidation potentials and barriers to conformational exchange in a family of porphyrin nanorings is used to deduce the aromatic stabilization energy.

2. INTRODUCTION

Aromaticity is one of the oldest and most important concepts in chemistry. It impacts a diverse range of molecular properties, such as thermodynamic stability, chemical reactivity, molecular geometry and magnetic susceptibility. This gamut of manifestations makes aromaticity difficult to define or quantify. One of the simplest definitions relates to magnetic behavior: An aromatic molecule sustains a ring current when placed in a magnetic field, and the direction of the current is such as to create a magnetic field opposing the external field inside the ring (i.e. it is diatropic). Antiaromatic molecules exhibit ring currents in the opposite (paratropic) direction, reinforcing the external field inside the ring. This definition is convenient to apply because the shielding effects of ring currents can be measured by NMR spectroscopy and modeled theoretically. The concept of aromatic ring currents was conceived by Pauling, Lonsdale and London during the 1930s⁵⁻⁷ and early work in this field has been extensively reviewed.⁸⁻¹⁰ The ring current I scales linearly with the external magnetic field B and is quantified by the ring current susceptibility (I/B in units of nA/T, sometime known as “ring current strength”, with the

convention that values are negative for diatropic currents). Here, we explore how aromatic and antiaromatic ring currents evolve as a function of ring size.

Hückel's rule is an excellent predictor of aromaticity: conjugated rings with $4n+2$ or $4n$ π -electrons are expected to be aromatic or antiaromatic, respectively. This rule was originally formulated for $[N]$ annulenes, i.e. monocyclic $(\text{CH})_N$ hydrocarbon rings, where N is even. It can also be applied to some polycyclic and heterocyclic systems; for example, it rationalizes the aromaticity of porphyrins, with circuits of 18 π -electrons. Most textbooks say that Hückel's rule only applies to molecules with up to about 22 π -electrons, and that larger rings do not exhibit aromaticity. In 1959, Longuet-Higgins and Salem¹¹ anticipated that [30]annulene would be non-aromatic and many subsequent theoretical studies predict that $[N]$ annulenes cease to have significant aromatic stabilization energy when $N > 22\text{--}30$.¹²⁻¹⁵ Many large π -conjugated macrocycles do not exhibit global (anti)aromaticity, as exemplified by the neutral **c-PN** nanorings discussed below. On the other hand, some large macrocycles exhibit global ring currents; for example, the ring currents in the molecules **1–12** (Figure 1) can be judged from the de-shielding of the external protons (H_{out}) and the shielding of the internal protons (H_{in}), observed in their ^1H NMR spectra.¹⁶⁻²⁷ The view that π -conjugated rings with >22 π -electrons are not aromatic is contradicted by these data and by the results on porphyrin nanorings which are the focus of this Account.

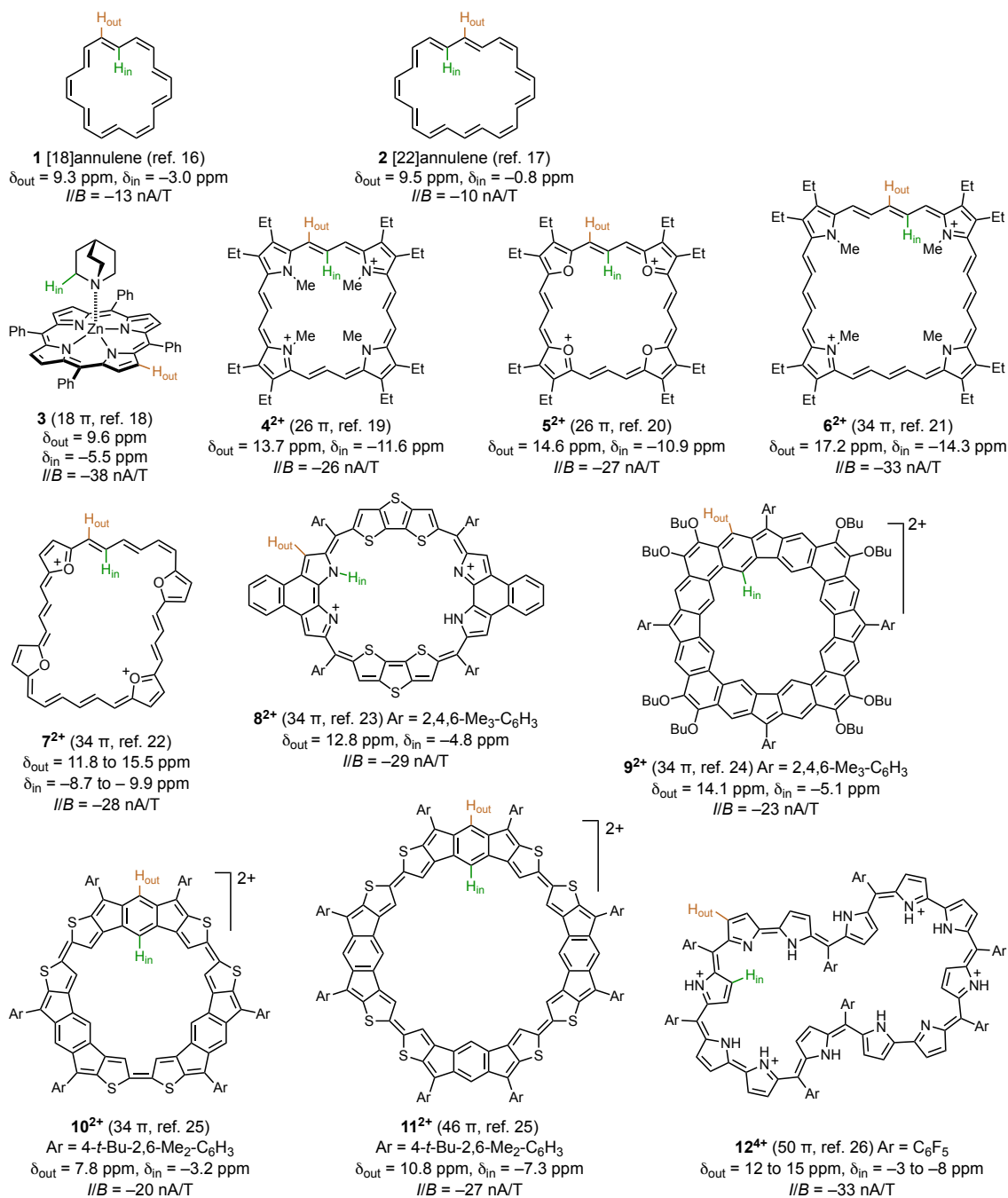


Figure 1. Examples of aromatic macrocycles with ¹H NMR chemical shifts for protons outside (H_{out}) and inside (H_{in}) the ring. Ring current susceptibilities (*I/B*) are estimated from experimental NMR data using Biot-Savart calculations as described in Section 5; see Supporting Information for details.

3. RING-CURRENTS IN PORPHYRIN NANORINGS

Butadiyne-linked cyclic porphyrin oligomers, **c-PN** ($N = 5-50$, where N is the number of porphyrins, Figure 2) are readily prepared by template-directed synthesis.²⁸⁻³⁰ These macrocycles are π -conjugated, as revealed by their absorption and fluorescence spectra,^{31,32} and they exhibit ultrafast excited state delocalization, like the rings of chlorophyll molecules that harvest sunlight for photosynthesis in some bacteria.³¹⁻³³ The neutral ground states are not globally aromatic, but oxidation to **c-PN**^{*Q*+}, reduction to **c-PN**^{*Q*-}, or optical excitation, gives rise to global aromatic or antiaromatic behavior.^{1,2,4,34-36}

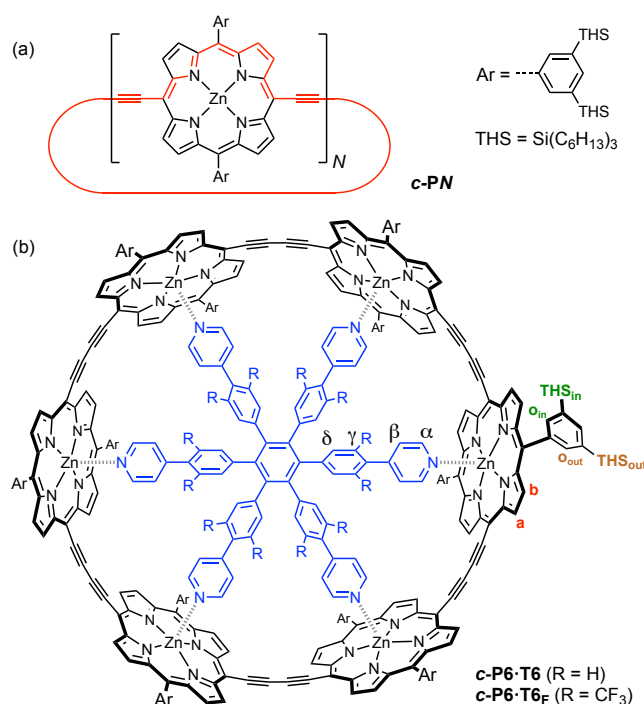


Figure 2. (a) General structure of butadiyne-linked porphyrin nanorings **c-PN**, with the pathway used for the Hückel electron count in red, and (b) structure of a six-porphyrin nanoring **c-P6** bound to a central template **T6** or **T6_F**.

The oligopyridyl templates used in the synthesis of porphyrin nanorings (e.g. **T6**, blue in Figure 2b) are valuable for studying the aromaticity of oxidized or reduced nanorings by NMR spectroscopy, because the resonances on the template probe shielding inside the nanoring. A

bound template also enables resonances from the porphyrins to be assigned, via the observation of nuclear Overhauser effects (NOEs) to the template. Fluorinated templates such as **T6_F** are particularly useful because they enable shielding to be probed by ¹⁹F NMR. The ¹H and ¹⁹F NMR spectra of **c-P6·T6_F^{Q+}** in oxidation states $Q = 0, 2, 4$ and 6 (Figure 3) provides strong evidence for global diatropic and paratropic ring currents.^{1,2} The following key features can be identified from these spectra:

- $Q = 0$, **c-P6·T6_F** (84 π ; non-aromatic): In the neutral state, each individual porphyrin has a normal aromatic ring current, as attested by the shielded α and β protons of the template, but there is no global ring current; the *ortho*-aryl protons o_{in} and o_{out} are almost coincident, as are the external and internal trihexylsilyl signals (THS_{in} and THS_{out}).
- $Q = 2$, **c-P6·T6_F²⁺** (82 π ; aromatic): The ¹H NMR spectrum is broad, but the ¹⁹F resonance is shielded compared with unbound **T6_F**, indicating a global diatropic ring current. The presence of a diatropic ring current is supported by the splitting between THS_{in} and THS_{out}, which were unambiguously assigned through observation of heteronuclear NOEs from THS_{in} to the CF₃ group.
- $Q = 4$, **c-P6·T6_F⁴⁺** (80 π ; antiaromatic): The α , β and δ template signals at 17–25 ppm indicate a large global paratropic ring current. This is confirmed by the wide splitting between THS_{in} and THS_{out} and by the shift of the ¹⁹F NMR signal.
- $Q = 6$, **c-P6·T6_F⁶⁺** (78 π ; aromatic): The ¹H NMR spectrum of the hexacation exhibits smaller shifts than the other oxidation states, but the o_{in}/o_{out} and THS_{in}/THS_{out} splittings indicate a global diatropic ring current, as confirmed by the ¹⁹F NMR signal.

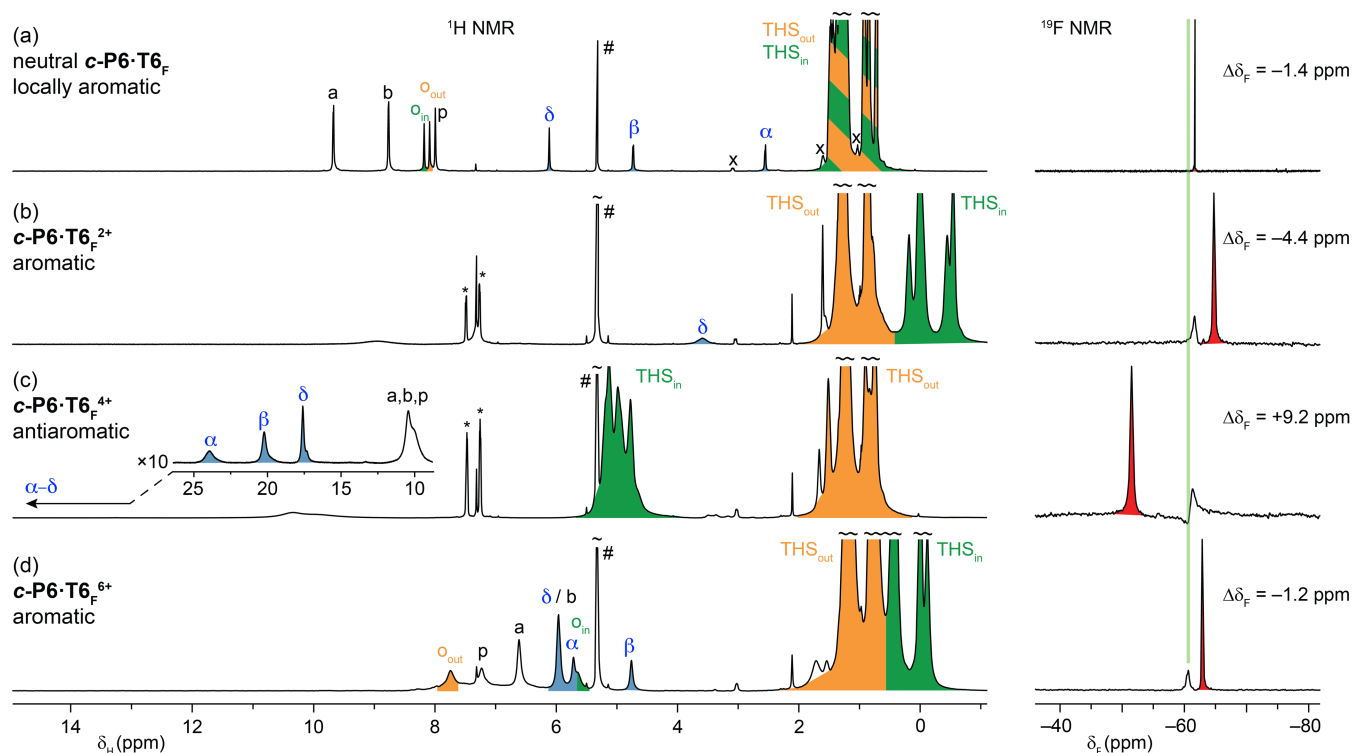


Figure 3. ^1H and ^{19}F NMR spectra (500 and 471 MHz, CD_2Cl_2) of neutral (a, 298 K) and oxidized (b, 253 K; c–d, 223 K) $\text{c-P6}\cdot\text{T6}_\text{F}$ generated by titration with thianthrenium hexafluoroantimonate; see Figure 2 for labeling. The green vertical line on the ^{19}F NMR spectra denotes the chemical shift of free T6_F ($\delta_\text{F} = -60.3$ ppm), which is the reference for $\Delta\delta_\text{F}$. Peaks labeled # and * arise from CHDCl_2 and neutral thianthrene, respectively; x denotes an unidentified impurity.

The Hückel π -electron counts listed above come from counting 10 electrons for each porphyrin unit and 4 for each butadiyne link (Figure 2a). In every case where a global ring current is apparent from the experimental NMR data, the direction of the current is correctly predicted by Hückel's rule.

The spectra in Figure 3 show that the direction of the ring current can be switched between aromatic and anti-aromatic by changing the number of π -electrons ($\Delta Q = 2$) by oxidation. Similar switches between aromatic and antiaromatic character are seen when the number of

electrons is changed by reduction ($c\text{-P6}\cdot\text{T6}^{4-}$ vs. $c\text{-P6}\cdot\text{T6}^{6-}$)³⁴ or by changing the size of the nanoring (e.g. $c\text{-P5}^{4+}$, $c\text{-P6}^{4+}$, $c\text{-P7}^{4+}$ and $c\text{-P8}^{4+}$)⁴ or by replacing a C₄ butadiyne link with a C₂ ethyne link.² The changes in magnetic shielding in homologous families of oligomers provide stronger evidence for global ring currents than studies on any single species. The antiaromaticity of $c\text{-P6}\cdot\text{T6}^{4+}$ and the aromaticity of $c\text{-P6}\cdot\text{T6}^{6+}$ are supported by magnetic susceptibility measurements, and $c\text{-P6}\cdot\text{T6}^{4+}$ is one of the few molecules with a strong enough paratropic ring current to result in net paramagnetism.^{1,37} Further experimental evidence for the aromaticity of $c\text{-P6}^{2+}$ and $c\text{-P6}^{6+}$, and the antiaromaticity of $c\text{-P6}^{4+}$, is provided by analysis of their redox potentials and conformational barriers from NMR exchange spectroscopy, which indicate an aromatic stabilization energy of around 1–5 kJ mol⁻¹.⁴ Similar global aromaticity has been reported in the 82 π -electron dication of a macrocyclic thiophene-linked porphyrin trimer.³⁸

The largest macrocycle yet to have been tested for redox-promoted global aromaticity is $c\text{-P12}$.² This nanoring can be fixed in a regular cylindrical geometry (5 nm diameter) by binding two extended fluorinated hexadentate templates T6e_F to form $c\text{-P12}\cdot(\text{T6e}_\text{F})_2$ (Figure 4a). ¹H, ¹³C and ¹⁹F NMR spectroscopy reveal global diatropic ring currents in the 6+ and 10+ oxidation states and a global paratropic current in the 8+ oxidation states, in agreement with Hückel's rule; $c\text{-P12}\cdot(\text{T6e}_\text{F})_2^{Q+}$: $Q = 6$, 162 π aromatic; $Q = 8$: 160 π antiaromatic; $Q = 10$: 158 π aromatic. No global ring current is detected in $c\text{-P12}\cdot(\text{T6e}_\text{F})_2^{12+}$, which illustrates a general trend: The global ring currents in $c\text{-PN}^{Q+}$ are strong in mixed-valence states, when $Q/N \approx 0.5$ and weak when $Q/N = 1$ (and negligible when $Q = 0$). The formation of a mixed valence state appears to enhance charge delocalization, just as a partially filled band is necessary for conduction in a metal.

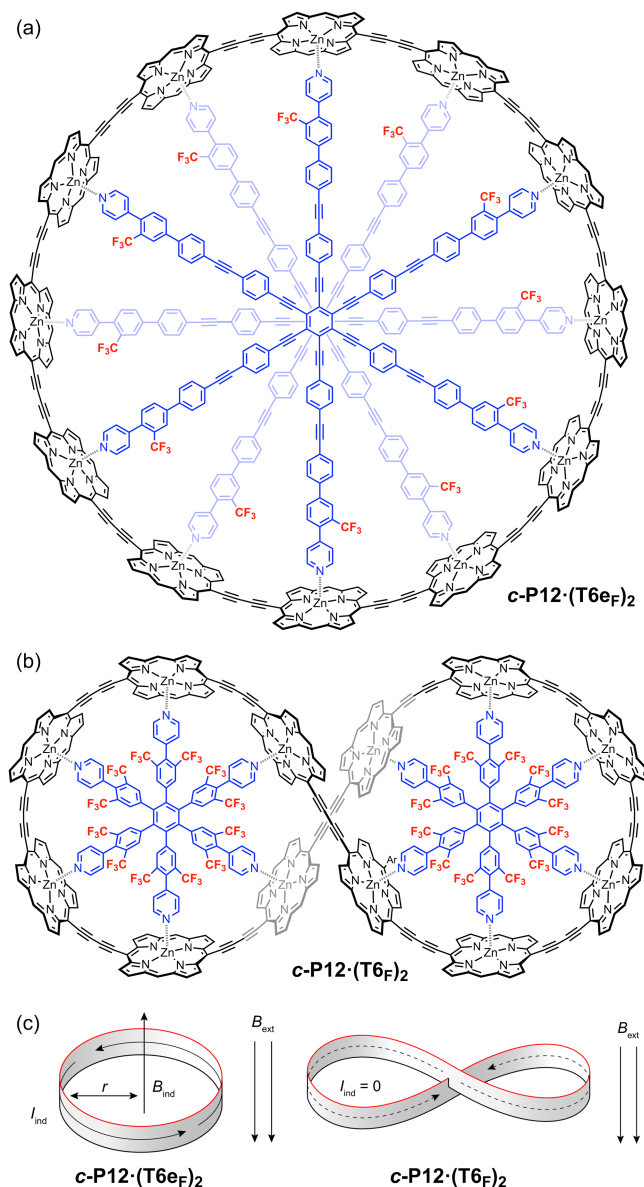


Figure 4. Structures of (a) $c\text{-P12} \cdot (\text{T6eF})_2$ and (b) $c\text{-P12} \cdot (\text{T6F})_2$, solubilizing sidechains omitted for clarity. The circular and lemniscate conformations are shown in (c).

Binding $c\text{-P12}$ to the small six-legged template T6_F gives a 1:2 complex $c\text{-P12} \cdot (\text{T6}_\text{F})_2$ (Figure 4b) with a figure-of-eight conformation, as established by NMR spectroscopy and X-ray crystallography.^{39,40} Fixing the nanoring into this lemniscate conformation is expected to block all global ring currents, because the current induced in one loop should be equal and opposite to that in the other loop (Figure 4c). In keeping with this simple picture, no global ring current is

detected in **c-P12**·(**T6_F**)₂^{Q+} in any oxidation state.² The suppression of ring currents in figure-of-eight shaped annulenes had been predicted theoretically,^{41,42} but was not observed experimentally in other figure-of-eight shaped aromatic systems,^{26,27,43} probably because they are not the right shape to achieve complete cancellation of the ring current.²

Optical excitation can also induce global aromaticity in porphyrin nanorings.³⁵ Baird's rule states that Hückel's rule is reversed in triplet T₁ excited states, so that rings with $4n$ π -electrons become aromatic, while those with $4n+2$ π -electrons are antiaromatic,⁴⁴⁻⁴⁶ and this rule is often applicable to singlet S₁ excited states.^{45,46} Thus the excited states of **c-P6** (84 π) and **c-P8** (112 π) are expected to be aromatic, whereas those of **c-P5** (70 π), **c-P7** (98 π) and **c-P9** (126 π) should be anti-aromatic. Alternating patterns in the fluorescence maxima and radiative rates in **c-PN**, when plotted as a function of N , provide experimental evidence for this phenomenon.³⁵

4. THEORETICAL SIMULATION OF RING-CURRENTS IN PORPHYRIN NANORINGS

Many computational techniques have been developed for predicting whether a molecule is aromatic.⁴⁷⁻⁵⁰ The most widely used approach, pioneered by Schleyer, is to model the shielding effects of ring currents by calculating the nucleus independent chemical shift (NICS) using DFT.⁴⁸ Positive and negative NICS values indicate deshielding and shielding, respectively. NICS values can be calculated at any point in space. For example, Figure 5 shows NICS_{iso} plotted across two orthogonal planes for **c-P6**^{Q+} for $Q = 0, 2, 4$ and 6 , calculated using the LC- ω hPBE ($\omega = 0.1$) functional.² These plots reproduce the shielding effects observed in the NMR spectra (Figure 3). The NICS plot for **c-P6**⁴⁺ has a low symmetry (C_2 rather than D_{6h}) reflecting the distortion expected in an antiaromatic ring (analogous to the D_{2h} geometry of cyclobutadiene).⁵¹

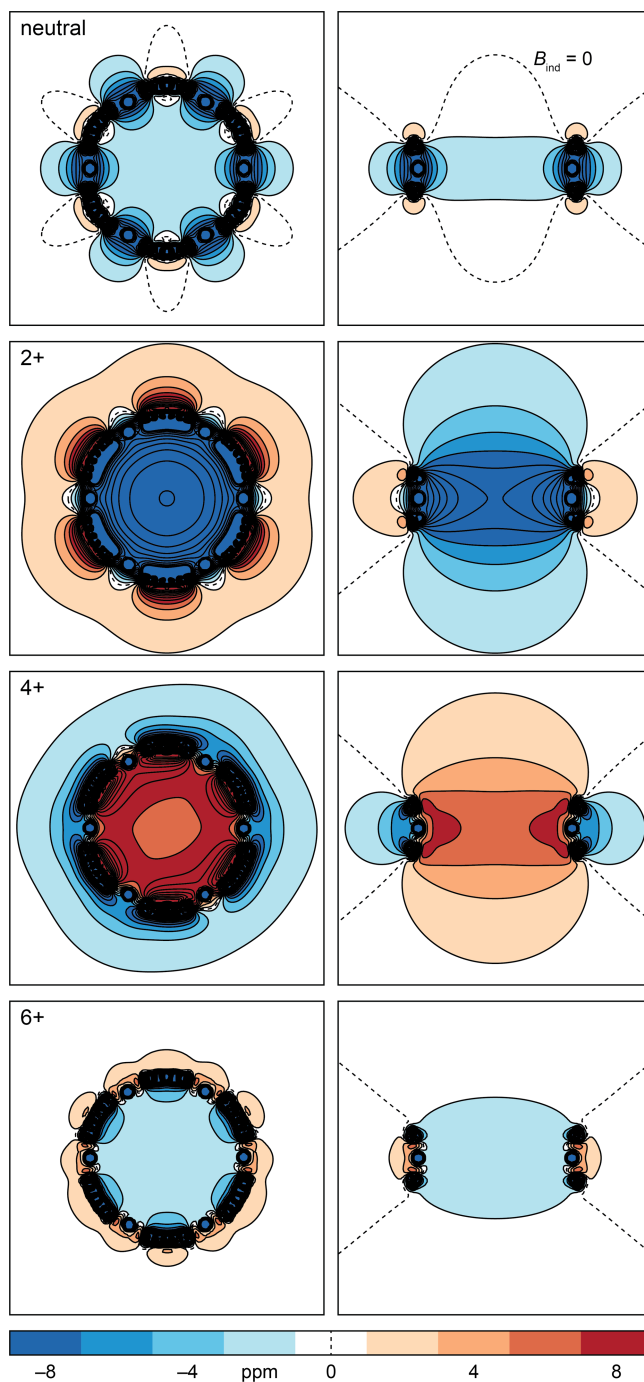


Figure 5. Plots of NICS_{iso} across two orthogonal planes for *c*-P6, *c*-P6²⁺, *c*-P6⁴⁺ and *c*-P6⁶⁺ calculated using LC- ω hPBE ($\omega = 0.1$). Geometries optimized with bound T6.

Various exchange-correlation functionals have been developed for DFT calculations, and the choice of functional can drastically affect the NICS results. Popular functionals such as B3LYP

tend to exaggerate electronic delocalization and global aromaticity in large molecules.^{35,52,53} This problem can be mitigated by using range-separated functionals such as LC- ω hPBE ($\omega = 0.1$), in which the amount of Hartree-Fock (HF) exchange changes as a function of distance.^{2,4,35,36,53} Changing the functional generally changes the magnitude of the NICS values, and in some cases it changes the direction of the predicted ring current.² We found that LC- ω hPBE ($\omega = 0.1$) generally gives NICS values that are consistent with experimental NMR shifts.^{2,4,36} Valiev, Baryshnikov and coworkers reported that the M06-2X functional, which includes a similar amount of HF exchange, reproduces the large positive magnetic susceptibility of **c-P6-T6**⁴⁺.³⁷ We typically used the double-zeta Pople-type 6-31G* basis set, but when studying porphyrin nanoring anions, we included diffuse basis functions (6-31+G*) for improved description of the less tightly-bound excess electrons.³⁴ Larger basis sets were not computationally affordable for molecules the size of porphyrin nanorings.

5. QUANTIFICATION OF RING CURRENTS FROM NMR DATA

Here we take a phenomenological approach and ask: If the changes in NMR chemical shift in an aromatic compound are attributed to a ring current, what ring current susceptibility (I/B) is most consistent with the experimental $\Delta\delta$ values? This question can be answered using the Biot-Savart law, which allows the magnetic field arising from a current, flowing between specified points, to be calculated at any point in space. Many authors have used Biot-Savart calculations to deduce ring currents from NMR data.⁵⁴⁻⁵⁷ Our method for implementing these calculations is detailed in the Supporting Information. In brief, it involves the following steps:

(i) $\Delta\delta$ values are calculated from experimental NMR data, using a range of probe nuclei (generally ¹H, ¹³C and ¹⁹F), by comparing NMR spectra of (anti)aromatic compounds with those of non-aromatic reference compounds.

(ii) The ground-state geometry of the molecule is calculated by DFT (B3LYP/6-31G*), starting from crystallographic coordinates if possible.

(iii) A current loop model is constructed, consisting of two circuits of infinitely thin wire 0.7 Å above and below the plane of the π -system.⁵⁵⁻⁵⁷ These current loops consist of discrete linear segments that follow the conjugated path of the molecule.

(iv) If the path of the current loop is planar, the z -axis is defined as perpendicular to this plane. The values of the induced magnetic field B_z at the locations of the probe nuclei are calculated using the Biot-Savart law, assuming a fixed ring current of 1 nA. These values of B_z are known as *ring current geometric factors* (RCGFs)⁵⁶ in units of $\mu\text{T/nA}$. RCGFs are purely geometrical factors, and if a macrocycle has several oxidation states with the same geometry, they have the same RCGFs, even if they have different ring currents. A planar ring current path is a valid approximation for most (anti)aromatic molecules, including all the molecules in Figure 1, except **12**⁴⁺, and all the porphyrin nanorings discussed here, except **c-P12**·(**T6_F**)₂. If the path is not planar, RCGF values are calculated as described in the Supporting Information.

(v) $\Delta\delta$ is plotted against RCGF, and the gradient of the straight line through the origin gives the ring current susceptibility, I/B , according to equation (1).

$$\Delta\delta = (I/B) \text{ RCGF} \quad (1)$$

The plot of $\Delta\delta$ vs. RCGF in Figure 6 is derived from the NMR spectra of **c-P6**·**T6_F** ^{Q^+} , where $Q = 2, 4$ or 6 (Figure 3). The excellent correlation shows that the data fit the ring current model. Fitting the NICS values in Figure 5 to the same model gives ring current susceptibilities of $I/B = -43, 47$ and -10 nA/T for the 2+, 4+ and 6+ oxidation states; these values agree reasonably with the experimental values of $-26, 61$ and -12 nA/T from NMR, respectively.

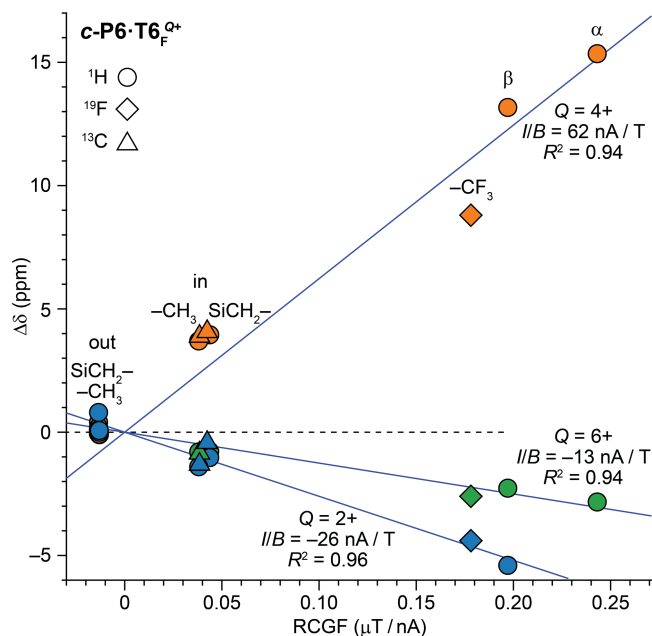


Figure 6. Experimental ring-current induced shifts ($\Delta\delta$) for ^1H , ^{13}C and ^{19}F signals in $c\text{-P6}\cdot\text{T6F}^{Q+}$ ($Q = 2, 4$ or 6) plotted against the RCGF from Biot-Savart calculations. (Data from spectra in Figure 3.)

Biot-Savart calculations, following the procedure outlined above and detailed in the Supporting Information, were used to calculate the ring current susceptibilities shown for the macrocycles in Figure 1 and the porphyrin nanorings shown in Figure 7.^{2,4} The message from these distributions of values is that ring current susceptibility does not have a strong dependence on ring size.

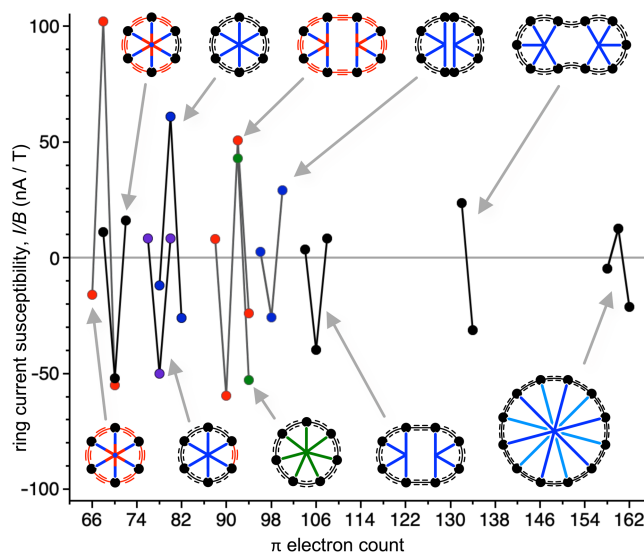


Figure 7. Plot of ring current susceptibility, I/B , from experimental NMR data, against the Hückel electron count for various porphyrin nanoring template complexes, each in several oxidation states. See Supporting Information for details of molecular structures and Biot-Savart calculations.

6. PERSISTENT CURRENTS IN MESOSCOPIC RINGS — MANIFESTATIONS OF AROMATICITY?

When a mesoscopic metal ring (diameter $\sim 200\text{--}1000$ nm) is placed in a magnetic field at low temperature, a *persistent current* flows around its circumference.⁵⁸ The direction of this current oscillates as a function of the field strength (B), with a period of a flux quantum $\phi_0 = h/e$, where h is the Planck constant and e is the elementary charge.⁵⁹ This means that the magnetic field for one cycle (B_0) is inversely proportional to the area of the ring, as expressed by equation (2), where r is the radius.

$$B_0 = \frac{\phi_0}{\pi r^2} \quad (2)$$

Oscillatory persistent currents have been detected in metal rings in the normal (i.e., non-superconducting) regime, as well as in rings of semiconductors such as indium-doped gallium

arsenide (diameter ~ 20 nm).⁶⁰ They are only observed when the coherence length of the electrons exceeds the circumference of the ring, which is why low temperatures are necessary (typically < 5 K). Theoretical calculations suggest that the sign of the persistent current depends on the number of delocalized electrons: a ring with $4n$ electrons is paramagnetic, whereas one with $4n+2$ is diamagnetic.⁶¹ This result is startlingly similar to Hückel's rule, but it has yet to be demonstrated experimentally for non-molecular rings.

It is easy to see why one would not expect to be able to observe field-dependent oscillations in the ring currents of aromatic molecules, even if they behaved like metal rings: From equation (2) a benzene molecule with a radius of 1.4 \AA would require a field of $B_0 \approx 10^4 \text{ T}$ for one cycle. The strongest static magnetic field available in a laboratory is about 45 T and an aromatic ring would need a radius of 5 nm (twice that of **c-P12**) to accommodate a flux quantum at this field. Although oscillatory ring currents have not yet been observed in molecules, they are predicted to occur in high magnetic fields.^{62,63} In the next paragraph, we explain how this prediction follows from Hückel molecular orbital theory.

If a magnetic flux ($\phi = B\pi r^2$) passes through a ring of delocalized electrons, it causes a shift in the phase of the wavefunction. This phase factor was used by London in the 1930s to calculate ring current effects in aromatic molecules, in his remarkably successful effort to extend Hückel's molecular orbital theory to explain the anomalously high magnetic susceptibility of benzene.⁷ For benzene, the simplest Hückel Hamiltonian has the form in equation (3). This Hamiltonian only includes the p_z orbitals and is limited to nearest-neighbor interactions. The diagonal elements α are the energy of the $2p_z$ orbital in carbon, and the off-diagonal elements β denote the resonance energy, which is responsible for bonding.

$$\mathcal{H} = \begin{bmatrix} \alpha & \beta & 0 & 0 & 0 & \beta \\ \beta & \alpha & \beta & 0 & 0 & 0 \\ 0 & \beta & \alpha & \beta & 0 & 0 \\ 0 & 0 & \beta & \alpha & \beta & 0 \\ 0 & 0 & 0 & \beta & \alpha & \beta \\ \beta & 0 & 0 & 0 & \beta & \alpha \end{bmatrix} \quad (3)$$

A magnetic field changes the Hückel resonance term (β), transforming equation (3) into (4),

$$\mathcal{H} = \begin{bmatrix} \alpha & \beta' & 0 & 0 & 0 & \beta'' \\ \beta'' & \alpha & \beta' & 0 & 0 & 0 \\ 0 & \beta'' & \alpha & \beta' & 0 & 0 \\ 0 & 0 & \beta'' & \alpha & \beta' & 0 \\ 0 & 0 & 0 & \beta'' & \alpha & \beta' \\ \beta' & 0 & 0 & 0 & \beta'' & \alpha \end{bmatrix} \quad (4a)$$

$$\beta' = \beta e^{2\pi i \frac{\phi}{N\phi_0}} \quad (4b)$$

$$\beta'' = \beta e^{-2\pi i \frac{\phi}{N\phi_0}} \quad (4c)$$

where $N = 6$ for benzene. The terms β' and β'' , with opposite phase shifts, correspond to moving an electron around the ring in opposite directions. More generally, for Hamiltonian matrix elements \mathcal{H}_{jk} where j and k are indices of adjacent atoms:

$$\mathcal{H}_{jk} = \beta e^{2\pi i \frac{BS_{jk}}{\phi_0}} \quad (5a)$$

$$S_{jk} = \frac{x_j y_k - x_k y_j}{2} \quad (5b)$$

where S_{jk} is the signed area of the triangle between the origin (the center of the ring) and the atoms j and k , such that $S_{jk} = -S_{kj}$.

The eigenvalues of equation (4) give the molecular orbital energies of equation (6), where l is a quantum number, as plotted in Figure 8a.

$$\varepsilon_{l,\phi} = \alpha + 2\beta \cdot \cos \left[\frac{2\pi}{N} \left(l - \frac{\phi}{\phi_0} \right) \right], \quad l = 0, \pm 1, \pm 2, \dots, (N/2) \quad (6)$$

At zero field, equation (6) gives the familiar Hückel molecular orbital configuration of benzene and the HOMO is a pair of degenerate filled orbitals ($l = \pm 1$). In contrast, at $\phi/\phi_0 = 0.5$, the electronic ground state has a half-filled degenerate pair of HOMOs, as expected for an *anti*-aromatic molecule. In effect, a flux of $\phi/\phi_0 = 0.5$ rotates the Frost-Musulin diagram by 30° (Figure 8a). The induced ring current is proportional to the gradient of the total energy of the system with respect to magnetic field (i.e., $I \propto \partial E/\partial B$) and I fluctuates between diatropic (negative) and paratropic (positive) with increasing field (Figure 8b). The plots in Figure 8a,b are derived from a simple Hückel-London model, but more sophisticated calculations give a similar result (Figure 8c,d).⁶³ This model predicts a sawtooth-like variation of the ring current, and calculations for mesoscopic metal rings make a similar prediction, but inclusion of thermal effects leads to a sinusoidal profile.⁶⁴ In this model, the magnetic field dependence of the electronic structure is a manifestation of the Aharonov-Bohm effect, because the field is confined entirely within the ring and so other effects that would arise from direct exposure of the atoms of the ring to the field are neglected.

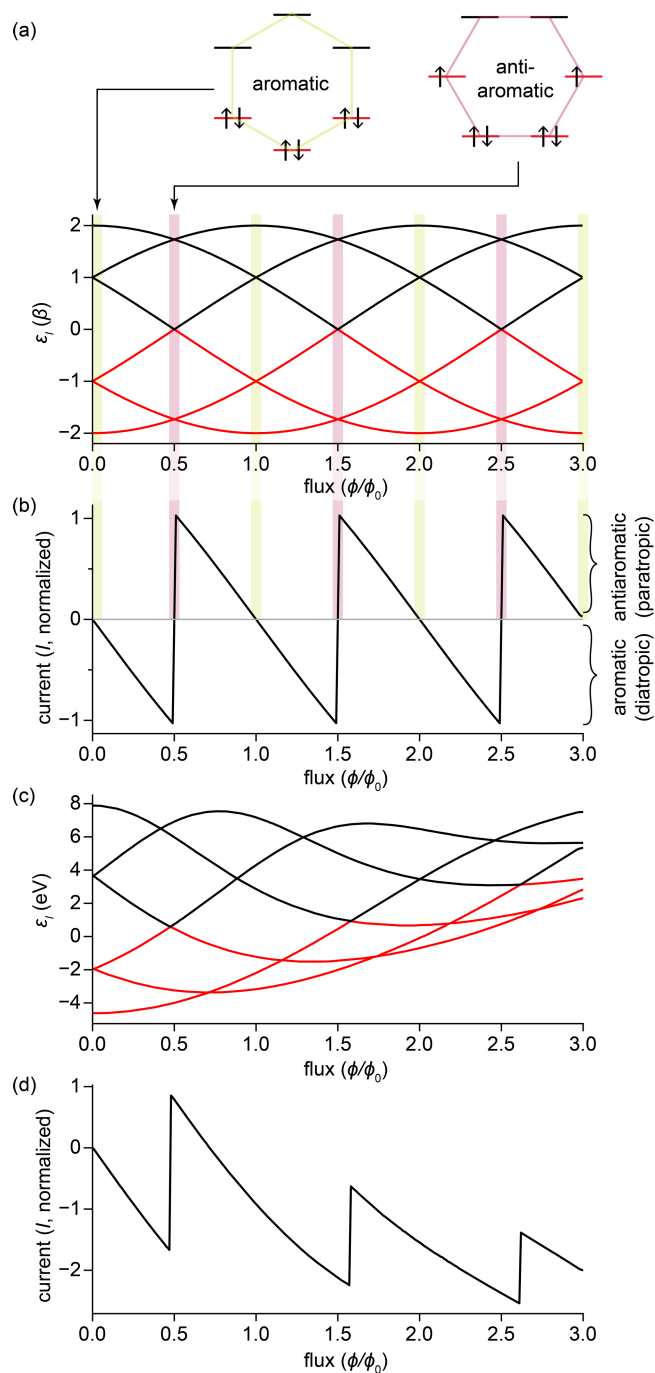


Figure 8. Simulations of the electronic structure (a and c) and magnetic moment (b and d) of benzene at high magnetic field, as a function of flux ϕ/ϕ_0 . Parts (a) and (b) are calculated using a simple Hückel-London model. In parts (a) and (c), occupied and unoccupied orbitals are colored red and black, respectively; in parts (b) and (d) the y-axis is normalized ring current, which is proportional to the orbital magnetic moment. Parts (c) and (d) are calculated using the screened-nuclei approximation (adapted from ref 63; copyright 2006 American Chemical Society).

The term *quantum ring* denotes an idealized structure in which a few mobile electrons are confined to a one-dimensional circular path, in such a way that the coherence of the wavefunction is preserved around the ring.^{65,66} Semiconductor rings with diameters of 20–300 nm are often described as quantum rings, and this model can be extended to any ring that supports a persistent current or an (anti)aromatic ring current. The electronic energy levels of a quantum ring arise directly from quantum confinement, and in the simplest case of a single electron, they are given by equation (7):

$$\varepsilon_{l,\phi} = \frac{\hbar^2}{2m_e r^2} \left(l - \frac{\Phi}{\Phi_0} \right)^2, \quad l = 0, \pm 1, \pm 2, \dots \quad (7)$$

where l is the angular momentum quantum number and m_e is the effective mass of the electron. This “particle-on-a-ring” model leads directly to a field-dependent oscillation in the total energy of the system (E), with a period of $B_0 = h/e\pi r^2$, and a corresponding oscillation in the ring current ($I \propto \partial E/\partial B$), just as predicted for a ring of discrete p_z orbitals by equation (6). The change in the electronic structure of a quantum ring caused by a magnetic field often results in measurable changes in the optical absorption and emission spectra, as well as changes in magnetic susceptibility associated with the persistent current.

The electronic structure of a quantum ring, at zero field, is similar to that of an (anti)aromatic molecule, with a single lowest energy level with no nodes ($l = 0$), followed by pairs of degenerate levels with increasing numbers of nodes ($l = \pm 1, \pm 2$, etc.). In some cases, scanning tunneling spectroscopy (STS) can be used to view the pattern nodes of these wavefunctions, by mapping the spatial distribution of the local density of states at specific bias voltages, by measuring the differential tunneling conductance (dI/dV) across the x,y -plane.^{67,68} This experiment has been carried out for a stack of two or three **c-P40** nanorings (diameter ≈ 17 nm) on a silver surface (Figure 9).³ The oxidation state of the nanoring was not measured in this

experiment, but there is probably some transfer of charge from the nanoring to the metal surface. Bright features are observed when the bias voltage is resonant with the energy of a molecular orbital. For example, at a bias voltage of -1.1 V, nine bright stripes become visible around the ring, and this pattern resembles the calculated probability distribution of HOMO-8, although it probably reflects the convolution of several molecular orbitals. These results suggest that there is coherent electronic delocalization around **c-P40** under the conditions of this experiment. According to equation (2), the magnetic field required for one flux quantum in **c-P40** is 18 T, which suggests that it may be possible to observe field-dependent oscillatory ring currents in this nanoring.

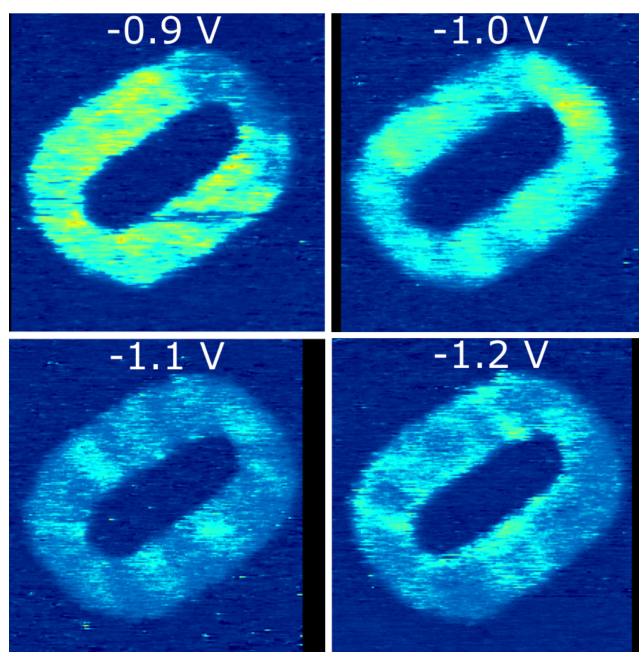


Figure 9. Differential conductance maps (dI/dV) for a stack of **c-P40** nanorings on Ag(111) under vacuum at ~ 78 K, at a bias of -0.9 to -1.2 V. The color scale indicates the differential tunneling conductance; image dimensions 28.4×23.5 nm. (Reproduced from ref. 3; copyright 2021 American Physical Society.)

7. CONCLUSIONS AND OUTLOOK

The results discussed in this Account show that aromaticity can arise in large macrocycles, with Hückel circuits of up to 162 π -electrons. There is a close similarity between aromatic ring currents and persistent currents in larger quantum rings, but it is not yet clear whether these two effects are the same, or just related. Experiments on large (anti)aromatic rings in high magnetic fields should resolve this issue. The idea of synthesizing π -conjugated macrocycles large enough to exhibit oscillatory ring currents at accessible magnetic fields was first proposed by Mayor and Didschies,⁶⁹ and it is still a fascinating challenge. If large enough (anti)aromatic rings can be prepared, we would expect to see dramatic changes in their NMR spectra as a function of magnetic field. When the flux through such a ring reaches about half a flux quantum ($\phi_0/2$), it would not just reverse the ring current; it would also cause a transformation in the electronic structure of the molecule. Thus we might expect to detect field-induced changes in chemical reactivity, as well as in the vibrational and electronic spectra. Magneto-optical effects may be easier to measure than changes in NMR spectra, since their measurement does not require the same degree of magnetic field homogeneity.

An important implication of the discovery of aromaticity in large macrocycles is that charge transport around the circumference of such molecules is phase-coherent. This means that if these molecules are connected between metal electrodes to form a metal|molecule|metal junction, one would expect to observe quantum interference between charge transport by the two pathways around the ring. If the pathways are identical, and there is no magnetic field, the two routes will be in phase giving constructive interference, but any difference between the paths, or magnetic flux, would create a phase difference, leading to destructive interference and blocking transport. Several prototypes for this type of molecular interferometer have been investigated,^{70,71} and

advances in nanotechnology will make the fabrication of these devices increasingly viable. Hod et al. predicted that the resistance of a molecular quantum ring in a metal|molecule|metal junction may be sensitive to weak magnetic fields corresponding to a small fraction of a flux quantum (e.g. $10^{-3} \phi_0$).⁷² Weak coupling to the leads allows the energy levels of the molecule to remain sharp, so that a small flux can shift these levels in or out of resonance with the leads, resulting in high sensitivity to magnetic field.

Finally, we should answer the question: Does aromaticity have a size limit? If persistent currents are a manifestation of aromaticity, then the size limit is a diameter of about 1 μm . Beyond this size, scattering breaks the phase coherence of the wavefunction, even at cryogenic temperatures.^{58,65,66} But what about molecular rings? This question is generally considered in the context of annulenes. No experimental NMR data are available for $[N]$ annulene with $N = 4n + 2$; $n > 5$, but theoretical studies predict that large annulenes undergo symmetry-breaking distortions leading to reduced π -conjugation,¹¹ analogous to the Peierls distortion in polyacetylene.⁷³ In linear conjugated polymers, the symmetry-breaking distortions that hinder charge transport can be partially overcome by doping. This is analogous to the promotion of global aromaticity in porphyrin nanorings through oxidation or reduction. Changing the oxidation state disrupts the local aromaticity of the individual porphyrin units and allows a global ring current to be established. It is also noticeable that the large aromatic macrocycles shown in Figure 1 are charged. What is the size limit of aromaticity in porphyrin nanorings? Two factors make it challenging to investigate aromaticity in doped nanorings larger than **c-P12**·(**T6eF**)₂ by NMR spectroscopy:

- (i) We need a template large enough to hold the macrocycle in an open conformation, to prevent conformational exchange between substituents inside and outside the ring. The

smaller oxidized rings $c\text{-P}N^{Q+}$, with $N = 5\text{--}8$, are rigid enough for their aromaticity to be probed without a template,⁴ but beyond this size, conformational exchange becomes fast on the NMR timescale unless the nanoring is bound to a template.

- (ii) In large nanorings, the redox potentials become closely spaced and oxidation or reduction generates mixtures of species with different oxidation states. Chemical exchange between different oxidation states is usually slow on the NMR timescale, enabling peaks from different oxidation states to be distinguished, so that this is not an insuperable problem.

The results summarized in Figure 7 suggest it will be possible to investigate aromaticity in larger nanorings, with Hückel circuits of more than 200 π -electrons and diameters greater than 10 nm.

It will also be interesting to measure the magnetic moments, or optical spectra, of single nanorings such as $c\text{-P40}^{Q+}$ on a surface, as a function of magnetic field, as demonstrated for non-molecular quantum rings.^{58,65,66} These experiments will be crucial for testing whether aromatic ring currents behave like persistent currents and for exploiting ring currents in molecular electronics.

ASSOCIATED CONTENT

Supporting Information.

The following files are available free of charge.

Details of Biot-Savart calculations (PDF)

AUTHOR INFORMATION

Corresponding Authors

*Email: michael.jirasek@org.chem.ethz.ch

*Email: harry.anderson@chem.ox.ac.uk

*Email: m.peek@unsw.edu.au

Notes

The authors declare no competing financial interest.

Biographies

Michael Jirásek completed his BSc and MSc at the University of Chemistry and Technology, Prague, including a year with François Diederich at ETH Zurich, Switzerland, before studying for his PhD in Oxford with Harry Anderson. He is currently a postdoctoral fellow with Helma Wennemers at ETH Zurich.

Harry L. Anderson received his PhD from Cambridge University, working with Jeremy Sanders, and pursued postdoctoral work with François Diederich at ETH Zurich. He has led an independent research group in Oxford since 1995.

Martin D. Peeks obtained his MChem from the University of St Andrews and completed his PhD in Oxford with Harry Anderson. He pursued postdoctoral work with Timothy Swager at MIT, USA, and was appointed to a faculty position at the University of New South Wales in 2019.

ACKNOWLEDGMENTS

We thank the ERC (Advanced Grants 320969 and 885606) and the EPSRC (grants EP/M016110, EP/R029229/1 and EP/N017188/1) for support. MDP thanks UNSW for a Scientia Fellowship.

REFERENCES

- (1) Peeks, M. D.; Claridge, T. D. W.; Anderson, H. L. Aromatic and antiaromatic ring currents in a molecular nanoring. *Nature* **2017**, *541*, 200–203.
- (2) Rickhaus, M.; Jirasek, M.; Tejerina, L.; Gotfredsen, H.; Peeks, M. D.; Haver, R.; Jiang, H.-W.; Claridge, T. D. W.; Anderson, H. L. Global aromaticity at the nanoscale. *Nat. Chem.* **2020**, *12*, 236–241.
- (3) Judd, C. J.; Nizovtsev, A. S.; Plougmann, R.; Kondratuk, D. V.; Anderson, H. L.; Besley, E.; Saywell, A. Molecular quantum rings formed from a π -conjugated macrocycle. *Phys. Rev. Lett.* **2020**, *125*, 206803.
- (4) Jirásek, M.; Rickhaus, M.; Tejerina, L.; Anderson, H. L. Experimental and theoretical evidence for aromatic stabilization energy in large macrocycles. *J. Am. Chem. Soc.* **2021**, *143*, 2403–2412.
- (5) Pauling, L. The diamagnetic anisotropy of aromatic molecules. *J. Chem. Phys.* **1936**, *4*, 673–677.
- (6) Lonsdale, K. Y. Magnetic anisotropy and electronic structure of aromatic molecules. *Proc. R. Soc. London. Ser. A - Math. Phys. Sci.* **1937**, *159*, 149–161.
- (7) F. London, Théorie quantique du diamagnetisme des combinaisons aromatiques. *C.R. Acad. Sci. (Paris)* **1937**, *205*, 28–30.
- (8) Lazzeretti, P. Ring currents. *Prog. Nucl. Mag. Res. Sp.* **2000**, *36*, 1–88.
- (9) Gomes, J. A. N. F.; Mallion, R. B. Aromaticity and ring currents. *Chem. Rev.* **2001**, *101*, 1349–1383.

- (10) Sundholm, D.; Fliegl, H.; Berger, R. J. F. Calculations of magnetically induced current densities: theory and applications. *WIREs Comput. Mol. Sci.* **2016**, *6*, 639–678.
- (11) Longuet-Higgins, H. C.; Salem, L. The alternation of bond lengths in long conjugated chain molecules. *Proc. R. Soc. London* **1959**, *251*, 172–185.
- (12) Dewar, M. J. S.; Gleicher, G. J. Ground states of conjugated molecules. II. Allowance for molecular geometry. *J. Am. Chem. Soc.* **1965**, *87*, 685–692.
- (13) Casademont-Reig, I.; Ramos-Cordoba, E.; Torrent-Sucarrat, M.; Matito, E. How do the Hückel and Baird rules fade away in annulenes? *Molecules* **2020**, *25*, 711.
- (14) Choi, C. H.; Kertesz, M. Bond length alternation and aromaticity in large annulenes. *J. Chem. Phys.* **1998**, *108*, 6681–6688.
- (15) Wannere, C. S.; Schleyer, P. von R. How aromatic are large $(4n + 2)\pi$ annulenes? *Org. Lett.* **2003**, *5*, 865–868.
- (16) Sondheimer, F. The annulenes. *Acc. Chem. Res.* **1972**, *5*, 81–91.
- (17) McQuilkin, R. M.; Metcalf, B. W.; Sondheimer, F. [22]Annulene. *J. Chem. Soc. D, Chem. Commun.* **1971**, 338–339.
- (18) Abraham, R. J.; Bedford, G. R.; McNeillie, D.; Wright, B. The NMR spectra of the porphyrins 16 — zinc(II) meso-tetraphenylporphyrin (ZnTPP) as a diamagnetic shift reagent. A quantitative ring current model. *Org. Magn. Reson.* **1980**, *14*, 418–425.
- (19) Gosmann, M.; Franck, B. Synthesis of a fourfold enlarged porphyrin with an extremely large, diamagnetic ring-current effect. *Angew. Chem., Int. Ed. Engl.* **1986**, *25*, 1100–1101.

- (20) Vogel, E.; Jux, N.; Dörr, J.; Pelster, T.; Berg, T.; Böhm, H.-S.; Behrens, F.; Lex, J.; Bremm, D.; Hohlneicher, G. Furan-based porphyrins: Tetraoxa[4n+2]porphyrin dications with 18 π -, 22 π -, or 26 π -electron systems. *Angew. Chem., Int. Ed.* **2000**, *39*, 1101–1105.
- (21) Knübel, G.; Franck, B. Biomimetic synthesis of an octavinylogous porphyrin with an aromatic [34]annulene system. *Angew. Chem., Int. Ed. Engl.* **1988**, *27*, 1170–1172.
- (22) Märkl, G.; Ehrl, R.; Kreitmeier, P.; Burgemeister, T. Superheteroaromaten mit Furan-Bausteinen: Isomere antiaromatische Tetraepoxy[36]annulene(6.4.6.4) und aromatische Tetraoxa[34]porphyrin(6.4.6.4)-Dikationen. *Helv. Chim. Acta* **2000**, *83*, 495–511.
- (23) Sarma, T.; Kim, G.; Sen, S.; Cha, W.-Y.; Duan, Z.; Moore, M. D.; Lynch, V. M.; Zhang, Z.; Kim, D.; Sessler, J. L. Proton-coupled redox switching in an annulated π -extended core-modified octaphyrin. *J. Am. Chem. Soc.* **2018**, *140*, 12111–12119.
- (24) (a) Lu, X.; Gopalakrishna, T. Y.; Phan, H.; Herng, T. S.; Jiang, Q.; Liu, C.; Li, G.; Ding, J.; Wu, J. Global Aromaticity in macrocyclic cyclopenta-fused tetraphenanthrenylene tettraradicaloid and its charged species. *Angew. Chem., Int. Ed.* **2018**, *57*, 13052–13056. (b) Gregolińska, H.; Majewski, M.; Chmielewski, P. J.; Gregoliński, J.; Chien, A.; Zhou, J.; Wu, Y.-L.; Bae, Y. J.; Wasielewski, M. R.; Zimmerman, P. M.; Stępień, M. Fully conjugated [4]chrysaorene. Redox-coupled anion binding in a tettraradicaloid macrocycle. *J. Am. Chem. Soc.* **2018**, *140*, 14474–14480.
- (25) Li, G.; Gopalakrishna, T. Y.; Phan, H.; Herng, T. S.; Ding, J.; Wu, J. From open-shell singlet diradicaloid to closed-shell global antiaromatic macrocycles. *Angew. Chem., Int. Ed.* **2018**, *57*, 7166–7170.

- (26) Soya, T.; Kim, W.; Kim, D.; Osuka, A. Stable [48]-, [50]-, and [52]dodecaphyrins(1.1.0.1.1.0.1.1.0.1.1.0): The largest Hückel aromatic molecules. *Chem. – Eur. J.* **2015**, *21*, 8341–8346.
- (27) Yoneda, T.; Soya, T.; Neya, S.; Osuka, A. [62]Tetradecaphyrin and its mono- and bis-Zn^{II} complexes. *Chem. Eur. J.* **2016**, *22*, 14518–14522.
- (28) Bols, P. N.; Anderson, H. L. Template-directed synthesis of molecular nanorings and cages. *Acc. Chem. Res.* **2018**, *51*, 2083–2092.
- (29) Liu, P.; Hisamune, Y.; Peeks, M. D.; Odell, B.; Gong, J. Q.; Herz, L. M.; Anderson, H. L., Synthesis of five-porphyrin nanorings by using ferrocene and corannulene templates. *Angew. Chem., Int. Ed.* **2016**, *55*, 8358–8362.
- (30) Kondratuk, D. V.; Perdigão, L. M. A.; Esmail, A. M. S.; O’Shea, J. N.; Beton, P. H.; Anderson, H. L. Supramolecular nesting of cyclic polymers. *Nat. Chem.* **2015**, *7*, 317–322.
- (31) Sprafke, J. K.; Kondratuk, D. V.; Wykes, M.; Thompson, A. L.; Hoffmann, M.; Drevinskas, R.; Chen, W.-H.; Yong, C. K.; Kärnbratt, J.; Bullock, J. E.; Malfois, M.; Wasielewski, M. R.; Albinsson, B.; Herz, L. M.; Zigmantas, D.; Beljonne, D.; Anderson, H. L., Belt-shaped π -systems: Relating geometry to electronic structure in a six-porphyrin nanoring. *J. Am. Chem. Soc.* **2011**, *133*, 17262–17273.
- (32) Parkinson, P.; Kondratuk, D. V.; Menelaou, C.; Gong, J. Q.; Anderson, H. L.; Herz, L. M. Chromophores in molecular nanorings - When is a ring a ring? *J. Phys. Chem. Lett.* **2014**, *5*, 4356–4361.

- (33) Yong, C.-K.; Parkinson, P.; Kondratuk, D. V.; Chen, W.-H.; Stannard, A.; Summerfield, A.; Sprafke, J. K.; O'Sullivan, M. C.; Beton, P. H.; Anderson, H. L.; Herz, L. M. Ultrafast delocalization of excitation in synthetic light-harvesting nanorings. *Chem. Sci.* **2015**, *6*, 181–189.
- (34) Peeks, M. D.; Jirasek, M.; Claridge, T. D. W.; Anderson, H. L. Global aromaticity and antiaromaticity in porphyrin nanoring anions. *Angew. Chem., Int. Ed.* **2019**, *58*, 15717–15720.
- (35) Peeks, M. D.; Gong, J. Q.; McLoughlin, K.; Kobatake, T.; Haver, R.; Herz, L. M.; Anderson, H. L. Aromaticity and antiaromaticity in the excited states of porphyrin nanorings. *J. Phys. Chem. Lett.* **2019**, *10*, 2017–2022.
- (36) Kopp, S. M.; Gotfredsen, H.; Deng, J.-R.; Claridge, T. D. W.; Anderson, H. L. Global aromaticity in a partially fused 8-porphyrin nanoring. *J. Am. Chem. Soc.* **2020**, *142*, 19393–19401.
- (37) Valiev, R. R.; Baryshnikov, G. V.; Nasibullin, R. T.; Sundholm, D.; Ågren, H., When are antiaromatic molecules paramagnetic? *J. Phys. Chem. C* **2020**, *124*, 21027–21035.
- (38) Ren, L.; Gopalakrishna, T. Y.; Park, I.-H.; Han, Y.; Wu, J. Porphyrin/quinoidal-bithiophene-based macrocycles and their dications: template-free synthesis and global aromaticity. *Angew. Chem., Int. Ed.* **2020**, *59*, 2230–2234.
- (39) O'Sullivan, M. C.; Sprafke, J. K.; Kondratuk, D. V.; Rinfrey, C.; Claridge, T. D. W.; Saywell, A.; Blunt, M. O.; O'Shea, J. N.; Beton, P. H.; Malfois, M.; Anderson, H. L. Vernier templating and synthesis of a 12-porphyrin nano-ring. *Nature* **2011**, *469*, 72–75.
- (40) Kondratuk, D. V.; Sprafke, J. K.; O'Sullivan, M. C.; Perdigo, L. M. A.; Saywell, A.; Malfois, M.; O'Shea, J. N.; Beton, P. H.; Thompson, A. L.; Anderson, H. L. Vernier-templated

synthesis, crystal structure, and supramolecular chemistry of a 12-porphyrin nanoring. *Chem. Eur. J.* **2014**, *20*, 12826–12834.

(41) Herges, R. Topology in chemistry: Designing Möbius molecules. *Chem. Rev.* **2006**, *106*, 4820–4842.

(42) Wirz, L. N.; Dimitrova, M.; Fliegel, H.; Sundholm, D. Magnetically induced ring-current strengths in Möbius twisted annulenes. *J. Phys. Chem. Lett.* **2018**, *9*, 1627–1632.

(43) Stępień, M.; Sprutta, N.; Latos-Grazyński, L. Figure eights, Möbius bands, and more: conformation and aromaticity of porphyrinoids. *Angew. Chem., Int. Ed.* **2011**, *50*, 4288–4340.

(44) Baird, N. C. Quantum organic photochemistry. II. Resonance and aromaticity in the lowest $^3\pi\pi^*$ state of cyclic hydrocarbons. *J. Am. Chem. Soc.* **1972**, *94*, 4941–4948.

(45) Rosenberg, M.; Dahlstrand, C.; Kilså, K.; Ottosson, H. Excited state aromaticity and antiaromaticity: Opportunities for photophysical and photochemical rationalizations. *Chem. Rev.* **2014**, *114*, 5379–5425.

(46) Oh, J.; Sung, Y. M.; Hong, Y.; Kim, D. Spectroscopic diagnosis of excited-state aromaticity: Capturing electronic structures and conformations upon aromaticity reversal. *Acc. Chem. Res.* **2018**, *51*, 1349–1358.

(47) De Proft, F.; Geerlings, P. Conceptual and computational DFT in the study of aromaticity. *Chem. Rev.* **2001**, *101*, 1451–1464.

(48) Chen, Z.; Wannere, C. S.; Corminboeuf, C.; Puchta, R.; Schleyer, P. v. R. Nucleus-independent chemical shifts (NICS) as an aromaticity criterion. *Chem. Rev.* **2005**, *105*, 3842–3888.

(49) Feixas, F.; Matito, E.; Poater, J.; Solà, M. Quantifying aromaticity with electron delocalisation measures. *Chem. Soc. Rev.* **2015**, *44*, 6434–6451.

(50) Gershoni-Poranne, R.; Stanger, A. Magnetic criteria of aromaticity. *Chem. Soc. Rev.* **2015**, *44*, 6597–6615.

(51) The plot for $c\text{-P6}^{6+}$ in Figure 5 also shows some distortion (D_{3h} rather than D_{6h}) and this probably relates to the weaker ring current. This distortion does not arise when the geometry is optimized with the B3LYP functional, which predicts a ground state with D_{6h} symmetry.¹

(52) Cohen, A. J.; Mori-Sánchez, P.; Yang, W. Insights into current limitations of density functional theory. *Science* **2008**, *321*, 792–794.

(53) Henderson, T. M.; Izmaylov, A. F.; Scalmani, G.; Scuseria, G. E. Can short-range hybrids describe long-range-dependent properties? *J. Chem. Phys.* **2009**, *131*, 044108.

(54) Waugh, J. S.; Fessenden, R. W. Nuclear resonance spectra of hydrocarbons: The free electron model. *J. Am. Chem. Soc.* **1957**, *79*, 846–849.

(55) Johnson, C. E.; Bovey, F. A. Calculation of nuclear magnetic resonance spectra of aromatic hydrocarbons. *J. Chem. Phys.* **1958**, *29*, 1012–1014.

(56) Haddon, R. C. The application of the Biot-Savart law to the ring current analysis of proton chemical shifts—I: A comprehensive investigation of the annulenes. *Tetrahedron* **1972**, *28*, 3613–3633.

(57) Monaco, G.; Zanasi, R. Assessment of ring current models for monocycles. *J. Phys. Chem. A* **2014**, *118*, 1673–1683.

(58) Bleszynski-Jayich, A. C.; Shanks, W. E.; Peaudecerf, B.; Ginossar, E.; von Oppen, F.; Glazman, L.; Harris, J. G. E. Persistent currents in normal metal rings. *Science* **2009**, *326*, 272–275.

(59) The magnetic flux quantum in a mesoscopic normal metal ring (h/e) is twice the magnetic flux quantum for an electron pair in superconductors ($h/2e$).

(60) Kleemans, N. A. J. M.; Bominaar-Silkens, I. M. A.; Fomin, V. M.; Gladilin, V. N.; Granados, D.; Taboada, A. G.; García, J. M.; Offermans, P.; Zeitler, U.; Christianen, P. C. M.; Maan, J. C.; Devreese, J. T.; Koenraad, P. M. Oscillatory persistent currents in self-assembled quantum rings. *Phys. Rev. Lett.* **2007**, *99*, 146808.

(61) Loss, D.; Goldbart, P. Period and amplitude halving in mesoscopic rings with spin. *Phys. Rev. B* **1991**, *43*, 13762–13765.

(62) Soncini, A.; Fowler, P. W. Non-linear ring currents: Effect of strong magnetic fields on π -electron circulation. *Chem. Phys. Lett.* **2004**, *400*, 213–220.

(63) Compernelle, S.; Chibotaru, L. F.; Ceulemans, A. Vortices and their relation to ring currents and magnetic moments in nanographenes in high magnetic field. *J. Phys. Chem. B* **2006**, *110*, 19340–19351.

(64) Cheung, H.-F.; Gefen, Y.; Riedel, E. K.; Shih, W.-H. Persistent currents in small one-dimensional metal rings. *Phys. Rev. B* **1988**, *37*, 6050–6062.

(65) Physics of Quantum Rings, Fomin, V. M., Ed., Springer, Berlin 2014.

(66) Viefers, S.; Koskinen, P.; Singha Deo, P.; Manninen, M. Quantum rings for beginners: energy spectra and persistent currents. *Physica* **2004**, *E21*, 1–35.

- (67) Pham, V. D.; Kanisawa, K.; Fölsch, S. Quantum rings engineered by atom manipulation. *Phys. Rev. Lett.* **2019**, *123*, 066801.
- (68) Su, J.; Fan, W.; Mutombo, P.; Peng, X.; Song, S.; Ondráček, M.; Golub, P.; Brabec, J.; Veis, L.; Telychko, M.; Jelínek, P.; Wu, J.; Lu, J. On-surface synthesis and characterization of [7]triangulene quantum ring. *Nano Lett.* **2021**, *21*, 861–867.
- (69) Mayor, M.; Didschies, C. A giant conjugated molecular ring. *Angew. Chem., Int. Ed.* **2003**, *42*, 3176–3179.
- (70) Vazquez, H.; Skouta, R.; Schneebeli, S.; Kamenetska, M.; Breslow, R.; Venkataraman, L.; Hybertsen, M.S. Probing the conductance superposition law in single-molecule circuits with parallel paths. *Nat. Nanotechnol.* **2012**, *7*, 663–667.
- (71) Li, Z.; Smeu, M.; Rives, A.; Maraval, V.; Chauvin, R.; Ratner, M.A.; Borguet, E. Towards graphyne molecular electronics. *Nat. Commun.* **2015**, *6*, 6321.
- (72) Hod, O.; Baer, R.; Rabani, E. Magnetoresistance of nanoscale molecular devices based on Aharonov-Bohm interferometry. *J. Phys.: Condens. Matter* **2008**, *20*, 383201.
- (73) Hoffmann, R. How chemistry and physics meet in the solid state. *Angew. Chem., Int. Ed. Engl.* **1987**, *26*, 846–878.